Old Dominion University

ODU Digital Commons

2015

Characterization of Terrestrial Dissolved Organic Matter Fractionated by pH and Polarity and Their Biological Effects on Plant Growth

Rachel L. Sleighter
Old Dominion University, RSleight@odu.edu

Paolo Caricasole

Kristen M. Richards

Terry Hanson

Patrick G. Hatcher
Old Dominion University, phatcher@odu.edu

Original Publication Citation

RESEARCH **Open Access**

Characterization of terrestrial dissolved organic matter fractionated by pH and polarity and their biological effects on plant growth

Rachel L Sleighter[1,2]*, Paolo Caricasole[1], Kristen M Richards[1], Terry Hanson[1] and Patrick G Hatcher[1,2]

Abstract

Background: Humic substances are ubiquitous in the environment, complex mixtures, and known to be beneficial to plant growth. To better understand and identify components responsible for plant growth stimulation, a terrestrial aquatic DOM sample was fractionated according to pH and polarity, obtaining acid-soluble and acid-insoluble portions, as well as acid-soluble hydrophobic and hydrophilic fractions using C18. The various fractions were characterized then evaluated for their biological effects on plant growth using bioassays with corn at two carbon rates.

Results: Approximately 43% and 57% of the carbon, and 31% and 69% of the iron, was found in the acid-insoluble and acid-soluble fractions, respectively. Upon separating the acid-soluble portion using C18 extraction, about 64% and 36% of the carbon (and 96% and 4% of the iron) was present in the hydrophilic and hydrophobic fractions, respectively. The acid-insoluble portion was more aromatic and less oxygenated than the acid-soluble fraction. The hydrophilic filtrate was oxygen-rich and contained mostly tannin-like molecules, while the hydrophobic retentate was more aromatic and lignin-like. During bioassay testing, it was found that more hydrophilic samples (those that are more oxygenated) yielded the highest response for shoot measurements. For root measurements, the lower DOC rate (0.01 mg/L C) gave better results than the higher DOC rate (0.1 mg/L C). Also, the hydrophobic, less oxygenated acid-insoluble sample performed better than the more hydrophilic acid-soluble portion. The polarity fractions at the lower carbon application showed that larger root systems occurred when there was more hydrophobic C18 retentate material present. The opposite was true for the root system at the higher carbon application, where larger roots existed when more hydrophilic C18 filtrate material was present.

Conclusions: Compositional differences were found when comparing the acid-soluble versus acid-insoluble portions and the hydrophobic versus hydrophilic C18 fractions, and activity with respect to plant stimulation was discerned. While a carbon rate affect was observed during foliar application to corn plants (with the lower carbon rate generally yielding the best biological stimulation), the various observed trends indicate that plant response is due to not only the amount of carbon present but also the type of carbon.

Keywords: Humic substances; Dissolved organic matter; C18 solid phase extraction; EEMs; FTICR-MS; Proton NMR; Plant growth; Bioassays

* Correspondence: rsleighter@fbsciences.com
[1]Research and Development, FBSciences, Inc, 4111 Monarch Way, Suite 408, Norfolk, VA 23508, USA
[2]Department of Chemistry and Biochemistry, Old Dominion University, Norfolk, VA 23529, USA

Sleighter *et al. Chemical and Biological Technologies in Agriculture* (2015) 2:9

Page 2 of 19

Background

Humic substances, which are ubiquitous in the environment, are present in varying amounts in all natural waters, soils, and sediments [1-3]. They are complex mixtures, containing thousands of individual molecules, all varying in their individual structure, function, reactivity, and polarity. Humic substances have long been regarded as beneficial to soil fertility and plant growth, and there are multiple excellent reviews on the subject that encompass decades of studies [4-6]. The positive outcomes are likely a combination of both direct and indirect effects, and humic substances have been shown to suppress the effect of pathogens and fungi, enhance lateral root development and root length/density, increase the cation exchange capacity and pH buffering capacity of soils, increase the availability and uptake of micronutrients, and promote growth and development via a hormone-like mechanism [7-13]. While there are many studies that have demonstrated improved plant health by treatment with humic substances, several questions remain, such as the best way to treat plants (seed vs. soil vs. foliar application), the rate/amount for treatment, and when to perform application(s), among numerous others. Because there are so many variables associated with the treatments on an agricultural level, there are sometimes conflicting and controversial results. It is likely that the optimal method and quantity for treatment varies depending on the crop, soil properties, and environmental conditions, as the mechanism for enhanced plant growth is uncertain.

Extensive chemical characterization of humic substances, and dissolved organic matter (DOM) in general, by use of advanced analytical techniques [14] has increased our understanding of the sources and composition of these complex mixtures. While numerous studies have highlighted the ability of humic substances (in general) to enhance plant response and growth parameters, the new challenge is to ascertain what portion or specific component(s) of the humic substances is most responsible for generating the positive response [15]. Nardi et al. [16] found that the lowest molecular weight portion of a humic acid fractionated by size exclusion chromatography was most active in stimulating plant metabolism, and this fraction was the most hydrophilic, containing more carbohydrates and less lignin-derived material, when compared to the larger size fractions. Other studies also found a link between hydrophobicity and plant response, but the more hydrophobic humic acids were those most active in plant response, with some humics acids increasing root length while others increased root density [17,18]. It is not uncommon for studies to present conflicting findings, especially when the various studies perform applications of the humic substances in different ways to different plants under different growing conditions, and also varying in concentration. It is clear that further research is needed to better understand the effects of humic substances on plants, especially as the use of humic substances for agricultural purposes is becoming more widely accepted and promoted.

Here, a terrestrial aquatic DOM sample was fractionated according to pH solubility and then polarity. The whole, original sample is available commercially from FBSciences, Inc. and has been shown to yield positive plant growth responses when utilized in agricultural applications. However, there is a need to identify what fractions of this DOM are most responsible for plant responses, so that we may employ further refinements to isolate and make available a more effective product. Thus, the whole sample was acidified to obtain the acid-insoluble and acid-soluble portions (similar to the method used by the International Humic Substances Society, [19]), and then, the acid-soluble portion was fractionated further into polar and non-polar fractions using C18 solid phase extraction (simulating that which occurs during reversed phase liquid chromatography, [20-22]). Material that passes through the C18 is polar, hydrophilic, and is referred to as the filtrate, while the material that is retained by the C18 (i.e., the retentate) is non-polar and hydrophobic [23]. The various fractions were chemically characterized using an array of advanced analytical techniques. Ultraviolet visible (UV/Vis) absorbance spectroscopy and excitation emission matrix spectroscopy (EEMs) were utilized to understand the optical properties of the chromophoric and fluorescent DOM [24,25]. To understand bulk chemical functionalities, liquid-state proton nuclear magnetic resonance (^{1}H NMR) spectroscopy was employed [26]. Finally, to obtain molecular-level information, electrospray ionization Fourier transform ion cyclotron resonance mass spectrometry (ESI-FTICR-MS) was used [27-29]. After characterization, the original whole and fractionated samples were subjected to plant bioassays at two carbon concentrations. Bioassays (performed *in vivo*) are utilized as a tool for measuring the effects of the different sample types on plant activity, in an effort to correlate molecular level details with plant response (i.e., root and shoot elongation, fresh and dry weights).

The two main goals of this study were to 1) chemically characterize the composition of the DOM fractionated according to pH solubility and polarity using a variety of advanced analytical techniques, and 2) demonstrate statistically significant responses upon treating plants with the fractionated samples in comparison to a control, in order to examine the influence that fractionation of the NOM has on plant growth and biological response.

Sleighter *et al. Chemical and Biological Technologies in Agriculture* (2015) 2:9

Page 3 of 19

Methods

Sample Fractionation

In this study, a terrestrial aquatic DOM sample was utilized for fractionation into various components. The source of the DOM is from fresh water in Northern Europe, and the final DOM product has been concentrated by a proprietary method and is commercially available from FBSciences, Inc. The "whole" sample was acidified drop-wise with 12 M HCl (trace metal grade, Fisher Scientific) to pH < 2. Precipitation was allowed to occur at room temperature for 40 hours. The sample was centrifuged to isolate the solid "acid-insoluble" portion from the liquid "acid-soluble" portion. The "acid-insoluble" solids were rinsed with acidified ultra-high quality (UHQ) water and freeze-dried to obtain a dry powder. The "acid-soluble" portion was fractionated further using C18 solid phase extraction (SPE, [30]), to obtain the hydrophobic retentate portion (i.e., what is retained by the C18 resin) and the hydrophilic filtrate portion (i.e., that which passes through the C18 resin). The C18 extraction disk (3 M Empore) was cleaned and activated using methanol (LC-MS grade, Fisher Scientific) and acidified UHQ water. The "acid-soluble" sample was passed through the C18 disk at a flow rate <25 mL/min, and the solution that passed through the resin was collected as the "filtrate". That which was adsorbed onto the resin was rinsed with acidified UHQ water and eluted off the resin with LC-MS grade methanol, to give the "retentate" portion.

Dissolved organic carbon (DOC) and Iron (Fe) Analysis

The C18 filtrate and retentate samples were rotary evaporated to remove methanol and replaced with UHQ water. The dried acid-insoluble fraction was re-dissolved in water amended with ammonium hydroxide (NH_4OH, final concentration 0.05%, pH 9). All fractions were then analyzed for their dissolved organic carbon (DOC) and iron (Fe) concentrations. Samples were analyzed for their DOC concentrations by high temperature catalytic combustion to CO_2 on a Shimadzu TOC-V_{CSN} total organic carbon analyzer calibrated with potassium hydrogen phthalate (Shimadzu). Samples were analyzed for their Fe content on a Perkin Elmer AAnalyst 200 Atomic Absorption Spectrometer calibrated with an iron reference standard solution (Fisher Scientific).

UV/Vis and EEMs Analysis

UV/Vis absorbance values were measured simultaneously as EEMs spectra were acquired on a Horiba Scientific Aqualog spectrophotometer with an excitation range of 240–600 nm at 3 nm intervals and an emission range of 213–623 at 3.368 nm intervals, with an integration time of 1 sec. All samples were analyzed at a range of DOC values (approximately 0.5-8 mg/L C), and

acquired spectra were corrected for their inner filter effects and Rayleigh masking using the Aqualog V3.6 software, which was also utilized for area integrations. Humic-like peaks A and C were integrated at [Ex 240–300 nm; Em 400–500 nm] and [Ex 300–360 nm; Em 400–500 nm], respectively, while peptide-like peak T was integrated at [Ex 240–300 nm; Em 250–350 nm] [12]. Specific UV absorption at 254 nm (SUVA254) was calculated based on the absorbance at 254 nm and the DOC concentration [31], and the fluorescence index (FI) was calculated from the ratio of emission intensity at 470:520 nm at excitation 370 nm [24,32].

Cation Exchange Resin Procedure

Because these samples contained a significant amount of Fe, cation exchange resin was utilized to prepare the samples for NMR and FTICR-MS, as these analyses are known to be hindered by the presence of paramagnetic species and ionic salts, respectively. The whole, acid-soluble fraction, and C18 filtrate were prepared using cation exchange resin (AG MP-50 resin, hydrogen form, 100–200 dry mesh size, Bio-Rad), similar to the guidelines established by the International Humic Substances Society [19]. The samples were prepared in batches, according to manufacturer guidelines, where the sample was added directly to the cleaned resin, stirred for 60 minutes, and then centrifuged to remove the resin from the sample. Using 3 steps of resin addition, 80-90% of the Fe was removed. It was not necessary to use the cation exchange resin on the acid-insoluble or C18 retentate samples, as these samples contained significantly less Fe.

NMR Analysis

The liquid-state ^1H NMR spectra were obtained on a 400 MHz Bruker Biospin Avance III NMR equipped with a broadband inverse probe using a water suppression pulse program (optimized WATERGATE pulse sequence [26]). This sequence suppresses the large peak due to water protons (at 4.7 ppm), allowing for the detection of protons from the natural DOM that would otherwise be obscured. This program also eliminates pre-concentration and re-dissolution steps that potentially lose an unknown portion of the DOM. The acid-insoluble sample was re-dissolved using sodium deuteroxide in D_2O diluted to pH 9 with UHQ water. All samples had a final sample composition of 90:10 H_2O:D_2O. Spectra were acquired with a 1 msec recycle delay and a time domain of 16 k, with 1000 scans (giving an approximate 1 hour analysis time). The scans were co-added and the summed free induction decay (FID) signal was exponentially multiplied and zero-filled once. The spectra were processed with a line broadening of 10 Hz.

Sleighter *et al. Chemical and Biological Technologies in Agriculture* (2015) 2:9

Page 4 of 19

For both NMR and FTICR-MS, the C18 filtrate and retentate samples were analyzed together in filtrate: retentate ratios of 100:0, 75:25, 50:50, 25:75, and 100:0. These ratios were also used during bioassays (described in detail below), in order to better understand how differing ratios of these two very different fractional components can influence plant response.

FTICR-MS Analysis

The samples prepared with cation exchange resin, described in the NMR section above, were also utilized for FTICR-MS analysis. The acid-insoluble sample was re-dissolved using UHQ water amended with NH_4OH (final concentration 0.05%, pH 9). All samples were diluted to give a final sample composition of 1:1 H_2O: MeOH and were continuously infused into an Apollo II ESI ion source (operating in negative ion mode) of a Bruker Daltonics 12 Tesla Apex Qe FTICR-MS using a syringe pump operating at 120 µL/hr. ESI voltages were optimized for each analysis using a spray shield voltage of 3.3-3.5 kV and a capillary voltage of 4.0-4.2 kV, yielding consistent and stable ESI spray shield and capillary currents of 180–210 nA and 20–30 nA, respectively. Ions were accumulated for 2–5 sec in a hexapole before being transferred to the ICR cell, where 300 transients, collected with a 4 MWord time domain, were added, giving about a 30–40 min total analysis time. The summed FID signal was zero-filled once and Sine-Bell apodized prior to fast Fourier transformation and magnitude calculation using the Bruker Daltonics Data Analysissoftware.

Prior to data analysis, all samples were externally calibrated with a polyethylene glycol standard and internally calibrated with fatty acids, dicarboxylic acids, and other naturally present compounds that are part of various CH_2 homologous series [33]. All m/z lists, created using a signal to noise threshold of 3, were exported for further analysis. Mass spectra were found to be reproducible, and the various samples were significantly different from one another when compared to instrumental duplicates of the same sample [34]. A molecular formula calculator generated empirical formula matches for all samples using carbon, hydrogen, oxygen, nitrogen, and sulfur with atomic ranges of $C_{5-50}H_{5-100}O_{1-30}N_{0-1}S_{0-1}$. Molecular formulae were assigned based on previously described rules [35], and the calculated theoretical m/z values of the assigned formulae agreed with measured m/z values with an error value of ≤ 0.5 ppm. For all samples, 82-92% of all peaks were assigned a unique molecular formula (excluding contributions from ^{13}C isotopes), and these formulae accounted for 91-97% of the summed total spectral peak magnitude. From the molecular formula assignments, average (by number and magnitude-weighted) mass spectral characteristics were calculated [23].

Statistical Analysis

In order to reveal the subtle differences among the NMR spectra and, separately, among the formulae assigned to FTICR-MS data, principal component analysis (PCA) was utilized. PCA, which assumes a linear relationship, reduces a multidimensional space into fewer dimensions, where the first dimension (i.e., the first principal component, PC1) explains the most variance. The second dimension (PC2), which is orthogonal to the first, explains most of the residual variance. The PCA output gives scores and loadings, which represent the projections of the samples and the variables, respectively, onto each PC. The loadings indicate that variable's contribution to the data variability along each PC. From these results, the samples and variables can be plotted on a two-dimensional PCA projection (a biplot), not only to group the samples according to their differences, but also to determine relationships between samples and variables. Data was compiled to create NMR and FTICR-MS matrices for each PCA.

The intensity values for the NMR spectra at 0.5-11 ppm were exported for each sample from the instrument at the resolution that the NMR measures, giving intensity values approximately every 0.0008 ppm, yielding 13,225 data points per sample. Because this level of resolution unnecessarily generates an excessively large dataset, an in-house written MatLab code was utilized to average across every 5 data points, giving a new resolution of 0.004 ppm and 2645 data points per sample. Data were normalized for each sample so that the summed total intensity equaled 1 for all samples.

For the FTICR-MS PCA, a data matrix was created for the samples and the complete set of unique CHO-only formulae using the relative magnitudes of the peaks. Relative magnitude is simply calculated by dividing the peak magnitude by the summed total peak magnitude for each sample. If a formula was not detected in that sample, a 0 was given in the matrix. Data were normalized for each sample so that the summed total magnitude equaled 1 for all samples, and PCA was conducted according to a previously published method [36].

Bioassays

Whole and fractionated samples were tested for plant response using a foliar application on corn (*Zea mays* L.) seeds treated with a pesticide package (to give healthy, pathogen-free seeds). Planting pots (18 cm diameter) filled with a vermiculite (grade 2, ULINE) substrate media were used, and 8 seeds were planted per pot. There were 3 replicate pots per treatment (including the control). Emergence was allowed to progress for 6 days,

Sleighter *et al. Chemical and Biological Technologies in Agriculture* (2015) 2:9

Page 5 of 19

and then seedlings were thinned (to allow more space for root growth), from 24 to 10 seedlings per treatment. The seedlings continued to grow for another 8 days, and then the foliar treatment was applied. The DOC concentrations of all 8 samples (whole, acid-insoluble, acid-soluble, and the 5 filtrate : retentate ratios of 100:0, 75:25, 50:50, 25:75, and 0:100) were normalized, and then 2 DOC rates were used for the foliar application: 0.01 and 0.1 mg/L C (UHQ water was used for the control). By using the same number of sprays from a hand sprayer containing the specified DOC value of each sample, 7 mL of each sample at each concentration were sprayed onto the plant foliage of each pot, ensuring adequate and uniform coverage of the plant leaves without inducing dripping or runoff of the product from the leaf margins. The plants continued to grow for another 7 days, and then the plants were harvested to evaluate their response to the treatment. Previous experiments (data not shown) have indicated that 7 days is the optimal amount of time post foliar application for this pot size. This time frame is long enough for the root system to grow and respond without the occurrence of root knotting but not so long that the plants become stressed due to the lack of macronutrients.

The entire growing period occurred in a greenhouse during the summer of 2014, where watering occurred on a daily basis. The following day/night program was used: day from 7 AM at 21–25°C with 50-60% humidity; night from 7 PM at 16–18°C with 50-60% humidity. Plants were not watered the day prior to harvesting, to allow the substrate media to partially dry. The plants were

extracted from the substrate, the roots were carefully washed to remove the vermiculite, and then fresh weight biomasses (for all seedlings of all replicates for each treatment taken together) were recorded. Then, the longest root and shoot of each individual seedling (for each replicate and each treatment) were measured to evaluate root and shoot elongation. The seedlings were then allowed to dry overnight in an oven at 60°C on aluminum foil, prior to taking dry masses of the full root and the full shoot systems for each seedling individually.

The assessment parameters were statistically evaluated by ANOVA single factor and Duncan's multiple range tests, to determine if each treatment is statistically different than the control and if the treatments are statistically different from one another, respectively. A value of $P = 0.05$ was chosen to determine the significance of the data (if $P > 0.05$ the data are not statistically different; if $P \leq 0.05$ the data are statistically different).

Results and Discussion
Carbon and Iron Concentrations
The fractionation scheme, along with the percentage that each fraction contributes to the whole, is represented in Figure 1. In terms of carbon, the acid-insoluble fraction was 43% of the whole, and the acid-soluble was 57%. The acid-soluble portion was then fractionated further, and the C18 hydrophilic filtrate accounted for 64% of the carbon in the acid-soluble portion, and the C18 hydrophobic retentate contained 36%. Based on iron, the acid-insoluble fraction was 31% of the whole, and
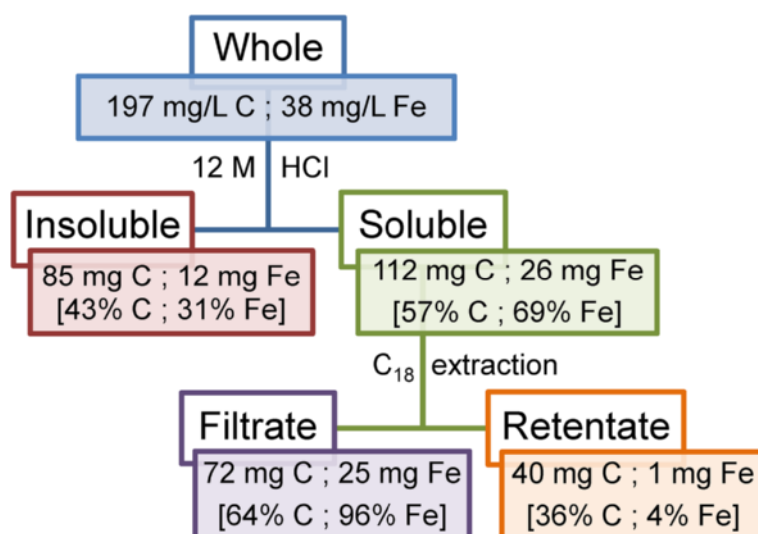
Figure 1 The analytical scheme utilized to fractionate the whole sample. After acidification, the acid-insoluble and acid-soluble components were isolated and then the acid-soluble portion was fractionated into its hydrophilic C18 filtrate and hydrophobic C18 retentate. The starting dissolved organic carbon and iron contents of the whole sample are given, along with the partitioning of carbon (and iron) between the fractions within each step.

Sleighter et al. Chemical and Biological Technologies in Agriculture (2015) 2:9

Page 6 of 19

the acid-soluble was 69%. The C18 hydrophilic filtrate accounted for 96% of the iron in the acid-soluble portion, and the C18 hydrophobic retentate contained 4%.

Characterization from Optical Measurements

Figure 2a shows the absorbance values across the entire wavelength range of 250–600 nm (for the samples analyzed at approximately 4–5 mg/L C). Typical of all DOM samples, absorbance values decrease with increasing wavelength, and there are no characteristic peaks [37]. Figure 2b shows the absorbance at 254 nm for each sample across the DOC range of 0.5-8 mg/L C. The whole and acid-insoluble samples have similar absorbance values, which are higher than the nearly identical absorbance values obtained for the acid-soluble and hydrophobic C18 retentate. The hydrophilic C18 filtrate has the lowest absorbance. Table 1 gives the SUVA254 values, and SUVA254 values are indicative of aromatic quality [31]. However, it should be noted that these SUVA254 values are somewhat higher that most natural waters, likely due to the high Fe content of the samples. FeIII absorbs at low wavelengths, which therefore inflates SUVA254 values [31]. The whole sample has the highest SUVA254 value, while the acid-insoluble portion has a higher SUVA254 value than the acid-soluble portion. The C18 retentate has a SUVA254 value higher than that of the filtrate.

Table 1 also gives the FI values, along with the percentages that humic-like peak A, humic-like peak C, and peptide-like peak T contribute to the total integrated fluorescence (for the samples analyzed at approximately 5 mg/L C). Higher SUVA254 and lower FI values are both indicators of aromaticity, with SUVA254 being indirectly proportional to FI. They are calculated from different parameters (SUVA254 using low wavelength adsorption and DOC concentration; FI using a ratio of higher wavelength fluorescence and is independent of DOC) and are often evaluated together, because FI is not subject to the same interferences as SUVA254 (e.g., Fe concentration). While Fe is known to quench fluorescence [25], FI is rarely affected by Fe concentrations because it is calculated by a ratio of emissions whose signals are decreased in the same manner. Corresponding with the SUVA254 values, the acid-insoluble portion has a lower FI than the acid-soluble sample, and the C18 retentate has a lower FI than the filtrate. While the whole sample had the highest SUVA254, its FI falls between the acid-insoluble and acid-soluble. The whole sample has the highest Fe concentration, inflating its SUVA254 value more severely than the other samples. However, in this case based on our results, FI seems to reveal the true trend of aromaticity amongst the fractionated samples, better than SUVA254.

Figure 2c gives the integrated Peak A areas from the EEMs analyses across the DOC range for all samples, while Figures 2d-f show the EEMs spectra for the whole, acid-insoluble, and acid-soluble samples. The whole and acid-soluble samples give quite similar EEMs spectra (which are also comparable to the hydrophobic retentate and hydrophilic filtrate samples whose spectra are not shown). The acid-insoluble sample appears to be somewhat different, with a wider (in the emission dimension) peak A (Ex 240–300 nm, Em 400–500 nm) and a less well defined peak C (Ex 300–360 nm, Em 400–500 nm). The hydrophobic retentate has the highest fluorescence, followed by the acid-soluble sample that fluoresces similarly to the whole sample, and the hydrophilic filtrate sample fluoresces slightly less than those. The acid-insoluble sample has the lowest fluorescence, but that is likely due to the fluorescence intensity of peak A being more widespread in this sample than in the others. As discussed above, Fe is known to increase absorbance values at low wavelengths as well as quench overall fluorescence [25]. This is likely why the hydrophobic retentate, that contains very little iron (Figure 1), has the highest fluorescence. The percentages that peaks A and C contribute to the total fluorescence are quite similar for all samples, with peak C being about 2/3 of that of peak A. Peak T (Ex 240–300 nm, Em 250–350 nm) is very low for all samples, as expected based on the terrestrial nature of these samples. This is consistent with the low FI values, which also indicate that there is little influence from microbial DOM.

Characterization from Proton NMR Measurements

Figure 3 shows the NMR spectra for the whole, acid-soluble, and acid-insoluble samples, as well as the various mixed ratios of the acid-soluble C18 filtrate : retentate (100:0, 75:25, 50:50, 25:75, and 0:100) samples. Peaks were integrated and their resulting areas are shown in Table 2. The peak at 0.0 ppm is tetramethylsilane (TMS), a reference standard added to the D_2O. It should be noted that in NMR, natural organic matter (NOM) samples give broad peaks due to high complexity. However, small molecules that are present in the NOM exist as sharp peaks (typically showing on top of the overlapping, broad NOM peaks). Acetic acid/acetate (H_3C-COOH, H_3C-COO$^-$) and formic acid/formate (HCOOH, HCOO$^-$), present in most dissolved NOM samples due to bacterial or photodegradation, give distinct peaks at approximately 2 and 8.3 ppm, respectively. Because these 'spikes' can alter the overall peak area integrations, giving false impressions of the total spectral intensity, they are excluded from the integration regions as marked in Table 2. Furthermore, the acetate and formate peaks appear slightly shifted from one sample to the next, because of the varying pH levels of these

Sleighter *et al. Chemical and Biological Technologies in Agriculture* (2015) 2:9

Page 7 of 19
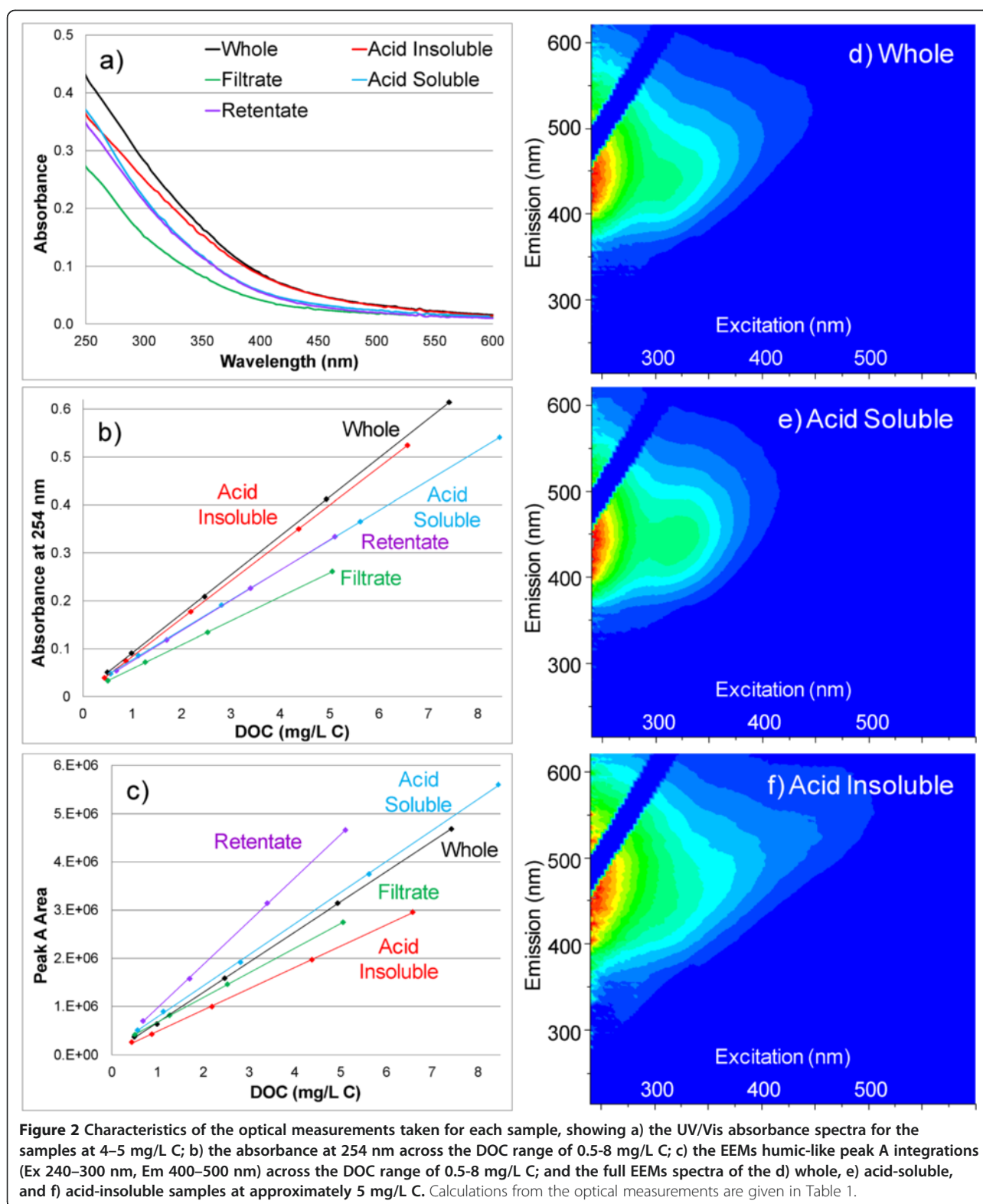
Figure 2 Characteristics of the optical measurements taken for each sample, showing a) the UV/Vis absorbance spectra for the samples at 4–5 mg/L C; b) the absorbance at 254 nm across the DOC range of 0.5-8 mg/L C; c) the EEMs humic-like peak A integrations (Ex 240–300 nm, Em 400–500 nm) across the DOC range of 0.5-8 mg/L C; and the full EEMs spectra of the d) whole, e) acid-soluble, and f) acid-insoluble samples at approximately 5 mg/L C. Calculations from the optical measurements are given in Table 1.

Sleighter *et al. Chemical and Biological Technologies in Agriculture* (2015) 2:9

Page 8 of 19

Table 1 Calculations from optical measurements of each sample

Sample	SUVA254 (L mg^{-1} m^{-1})	FI	EEMs Peak Areas		
			% A	% C	% T
Whole	8.35	1.34	61%	37%	2%
Acid insoluble	8.00	1.13	62%	35%	3%
Acid soluble	6.50	1.40	59%	39%	2%
C18 filtrate	5.16	1.44	56%	41%	2%
C18 retentate	6.53	1.29	61%	36%	3%

SUVA254: specific ultraviolet absorbance at 254 nm.
FI: fluorescence index, emission ratio of 420:520 nm at excitation 370 nm.
Peak A: 240–300 nm Ex; 400–500 nm Em.
Peak C: 300–360 nm Ex; 400–500 nm Em.
Peak T: 240–300 nm Ex; 250–350 nm Em.
Absorbance and EEMs fluorescence spectra are shown in Figure 2.

samples that allow these compounds to exist in both their ionic (i.e., acetate and formate) and protonated (i.e., acetic acid and formic acid) forms. For example, because the whole and acid-soluble samples are acidic (due to their preparation with the cation exchange resin), the formic acid peak is up-field of the formate peak that exists in the basic, acid-insoluble sample (Figure 3a). While methanol is also a natural biodegradation product, a small amount of residual methanol likely exists in the C18 samples, as the methanol spike at about 3.4 ppm in the C18 samples increases as more of the retentate fraction exists in the samples where ratios of filtrate : retentate are mixed (Figure 3b).

Based on the NMR spectra and area integrations, the acid-soluble sample is more oxygenated (2–5 ppm), whereas the acid-insoluble portion contains more olefins and aromatics (5–9 ppm). For the C18 samples, as the ratio of filtrate : retentate goes from 100:0 to 0:100, the aliphatic and aromatic components both increase, while the oxygenation decreases. While there is much overlap of the samples across the entire chemical shift range, the subtle differences amongst the spectra are revealed by utilizing PCA.
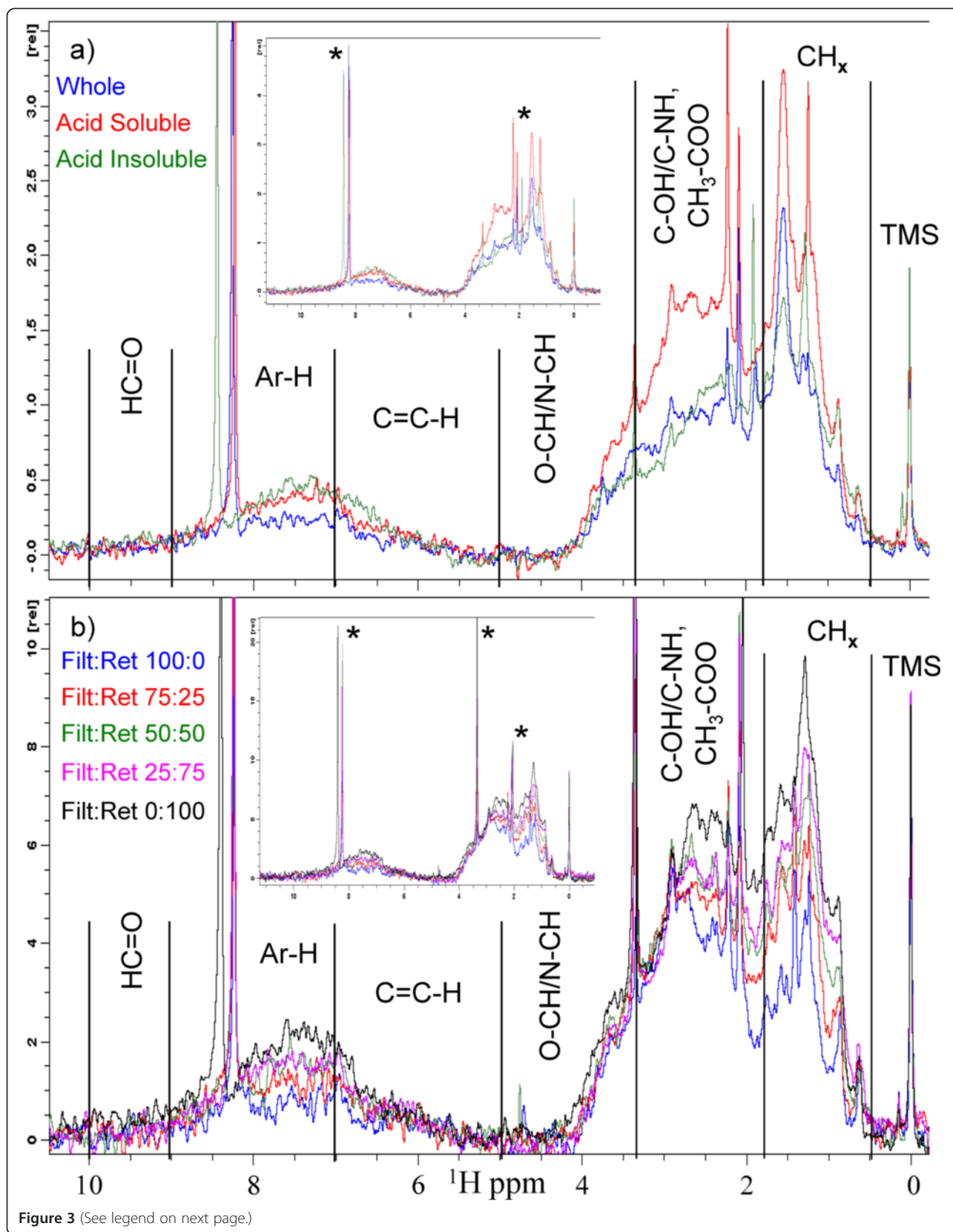
The original PCA executed on the NMR data revealed that statistical differences were primarily driven by the pH affect. Acidic samples were enriched in acetic acid and formic acid, while neutral/basic samples were enriched in acetate and formate. The presence or absence of methanol was also driving the PCA (particularly for the C18 samples). Because these small molecules exist as sharp peaks in the spectra, they are the first (and largest) differences found by PCA. Thus, a data matrix was created for a new PCA, ignoring certain regions of the NMR spectra. The following areas were deleted: >8 ppm, 3.2-4 ppm, and 1.8-2.4 ppm, to remove the areas of the spectrum that depend on pH, as well as the

methanol peak. The subsequent NMR PCA matrix had a dimension of 8 (samples) x 1537 (NMR intensity values as variables).

Figure 4 shows the PCA biplot of the samples' scores, along with the NMR spectra that have been reconstructed using the PC1 and PC2 variable loadings. PC1 explains 57% of the variance of the 1537 variables among the 8 samples, with PC2 explaining an additional 31% of the variance. The C18 fractionated samples all have positive PC1 scores, while the whole, acid-insoluble, and acid-soluble have negative PC1 scores. PC2 separates the acid-insoluble from the whole and acid-soluble samples, as well as the hydrophobic retentate from the hydrophilic filtrate.

The reconstructed NMR spectra elucidate the reasons for the sample groupings. From the PC1 loadings (Figure 4b), it is clear that the large aliphatic peak at about 1.5 ppm versus the oxygenated region at 2.4-3.2 ppm are the main factors driving the PC1 variance. Because the peak at 1.5 ppm has a negative PC1 loading, it is enhanced in the whole, acid-insoluble, and acid-soluble samples (as they have negative PC1 scores). The whole and acid-insoluble samples are more enriched in the peak at 1.5 ppm than in the oxygenated region (as they have larger negative PC1 scores). However, the acid-soluble sample has both of these regions at quite high intensities, giving a PC1 score that is closer to 0 (but still negative). The peak at 1.2 ppm (which is defined in all samples, Figure 3) is due to CH_x protons on aliphatic chains, while the peak at 1.5 is likely due to aliphatic protons that are attached to carbons that are next to either an olefin group or a carboxyl group ($H_2C = CH$-CH_2-R; HOOC-CH_2- CH_2-R). It is clear that this aliphatic peak at 1.5 ppm is more prevalent in the samples fractionated by pH and less so in the C18 samples (Figure 3). Because this peak is prevalent in the acid-soluble sample, we would also expect to detect it in the polarity-separated samples. It is likely that this region is less defined in the C18 samples, because these types of functionalities partition between the hydrophobic retentate and hydrophilic filtrate depending on the composition of the R group. The presence of a well-defined peak at 1.5 ppm in the acid-soluble sample and the lack there of in the C18 samples leads to their separation in the PC1 dimension.

The C18 samples (with positive PC1 scores) are more enriched in the oxygenated region at 2.4-3.2 ppm (as this region has positive PC1 loadings) than in the peak at 1.5 ppm. Furthermore, the oxygenation degree increases as more of the filtrate sample is present in the mixed ratios of C18 filtrate : retentate. These observations are in agreement with the expected mechanism of the extractions, where polar species (i.e., those that are more oxygenated) are not adsorbed to the resin and thus remain

Sleighter *et al. Chemical and Biological Technologies in Agriculture* (2015) 2:9

Page 9 of 19

Figure 3 (See legend on next page.)

Sleighter *et al. Chemical and Biological Technologies in Agriculture* (2015) 2:9

Page 10 of 19

in the filtrate portion. However, the C18 samples do not simply increase horizontally in the PC1 dimension, but rather on a diagonal, meaning that their differences are a combination of PC1 and PC2 variance.

In the PC2 dimension, the main drivers of the variance (Figure 4c) are the peak at 1.5 ppm and the oxygenated region at 2.4-3.2 ppm versus the aromatic region at 7–8 ppm and the aliphatic region at 0.5-1.2 ppm. The acid-insoluble sample has a very low PC2 score, indicating that it is particularly enriched in the aromatic region, as well as aliphatic CH_x functionalities. The other samples are more oxygenated (Figure 3, Table 2), giving higher PC2 scores. The samples with higher C18 filtrate portions having higher PC2 scores are more enriched in the oxygenated area, while the C18 retentate-dominated samples with lower PC2 scores are enriched in the aromatic and CH_x aliphatic (0.5-1.2 ppm) areas. In this PC2 dimension, the acid-soluble sample score falls between the 50:50 and 75:25 filtrate : retentate ratio sample scores, as expected based on the relative proportions of the filtrate and retentate in the original acid-soluble sample (Figure 1).

Characterization from FTICR-MS Measurements

All of the acquired FTICR mass spectra were similar to DOM samples analyzed previously [14,23,33-36,38], with most peaks existing at 300–600 m/z. The majority of peaks appear at odd m/z values, and, based upon the nitrogen rule, indicate a predominance of zero or an even number of nitrogens in the molecules. Peaks at even nominal masses are those that contain either an odd

number of nitrogen atoms or are ^{13}C isotopes of the ^{12}C peaks at the previous nominal mass [39]. The presence of the ^{13}C isotopes 1.0034 m/z units away from their corresponding ^{12}C peaks indicate that the ions are singly charged [39,40]. Numerous peaks (up to 25) were detected at each nominal mass, indicating the complexity of each sample. The formula assignments showed that the vast majority of compounds contain only C, H, and O (64-84% by number and 84-91% by magnitude), with less contribution from N and S (Table 3). There are very few formulae containing both N and S together (<1% of the total number and summed total spectral magnitude), and formulae that do contain both N and S correspond to low magnitude peaks with S/N ratios near the threshold value of 3.

The whole and acid-soluble samples are very similar with regard to their averaged elemental ratios and heteroatom composition, with the acid-insoluble material containing the highest amount of CHO-only formulae, indicating that the heteroatoms are less likely to precipitate, especially sulfur-containing components (Table 3). The C18 filtrate contains more heteroatoms than the C18 retentate (which is consistent with previous studies [23,30,36], as these polar species are not adsorbed to the C18 resin, especially the sulfur species (which are typically also associated with high oxygenation, such as sulfates, and are very polar). Also in Table 3 are the number-averaged and magnitude-weighted calculations. Again, the whole and acid-soluble samples are quite similar. The acid-insoluble sample has a much lower O/C average and an H/C average that is slightly higher than

Table 2 Proton NMR peak area integrations at the given ppm ranges, for each sample

Sample	CH_x	Total aliphatic	#C-OH/ C-NH	O-CH/ N-CH	Total oxygenated	C = C-H	*Ar-H	*Total aromatic	O = C-H
	0.5-1.8	0.5-1.8	2.0-3.3	3.4-5	2-5	5-7	7-9	5-9	9-10
Whole	43.0	**43.0**	30.4	7.0	**37.4**	5.5	12.3	**17.8**	1.8
Acid insoluble	38.9	**38.9**	28.0	6.8	**34.8**	7.1	16.7	**23.8**	2.5
Acid soluble	38.7	**38.7**	36.5	7.6	**44.1**	4.9	11.2	**16.1**	1.1
C18 Fil:Ret 100:0	30.4	**30.4**	42.3	8.5	**50.8**	6.3	11.3	**17.6**	1.2
C18 Fil:Ret 75:25	33.5	**33.5**	38.8	7.3	**46.1**	6.0	13.2	**19.2**	1.2
C18 Fil:Ret 50:50	36.2	**36.2**	34.5	7.1	**41.6**	6.4	14.6	**21.0**	1.2
C18 Fil:Ret 25:75	40.2	**40.2**	32.3	5.2	**37.5**	6.2	15.0	**21.2**	1.1
C18 Fil:Ret 0:100	41.2	**41.2**	30.3	5.3	**35.6**	6.3	15.9	**22.2**	1.0

#integration region excludes the peak area for acetate/acetic acid.
*integration region excludes the peak area for formate/formic acid.
Values given in bold are for the summed total peak areas in the aliphatic, oxygenated, and aromatic regions.
The ^{1}H NMR spectra are shown in Figure 3.

Sleighter *et al. Chemical and Biological Technologies in Agriculture* (2015) 2:9

Page 11 of 19

Figure 4 Results of the principal component analysis of the NMR data, showing a) the samples' scores, as well as the reconstructed NMR spectra according to the b) PC1 and c) PC2 loadings. Bulk functionalities by chemical shift are given.
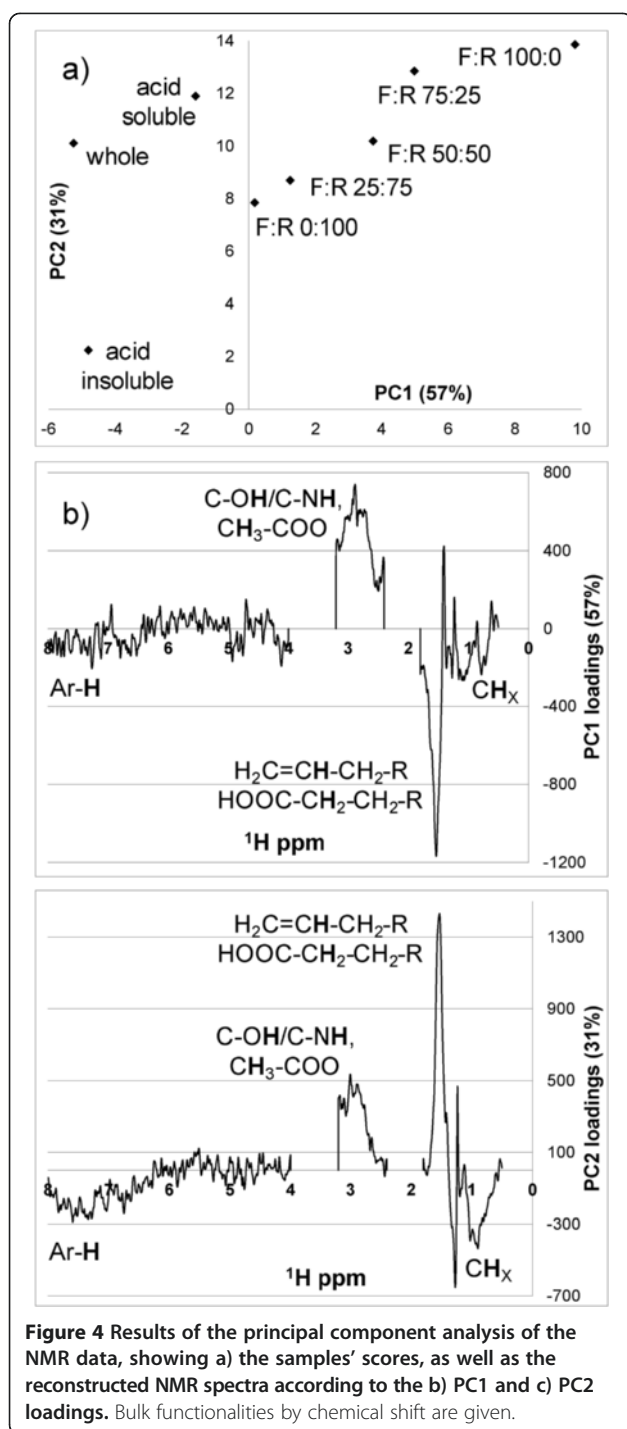
the whole and acid-soluble samples. These values indicate that the precipitated acid-insoluble material contains components with very little oxygenation. As the sample progresses from filtrate to retentate, the average O/C and DBE/C ratios decrease. This indicates that the filtrate is more oxygenated and less aromatic than the retentate portion. These averaged mass spectral characteristics agree quite well with the optical and NMR results.

From the molecular formula assignments, van Krevelen diagrams [41] were created, where molar O/C ratios are plotted against molar H/C ratios (Figure 5). From these diagrams, one can parse the formulae by regions of the van Krevelen diagram that denote molecular similarities with groups of compounds such as lipid, lignin, tannin, or condensed aromatics [42-44]. The whole and acid-soluble samples encompass all of these regions, giving van Krevelen diagrams that are very similar to one another (Figure 5a and b). The formulae in the acid-insoluble portion exist mostly at low O/C in the condensed aromatic and lipid regions, with some points aligning in the low O/C lignin-like region (Figure 5c). This van Krevelen diagram of the acid-insoluble fraction is similar to those of other types of humic acids [43,45]. There are many formulae aligning in the lipid-like region of the acid-insoluble sample, and because this was precipitated material from the whole, we would have expected to observe this cluster of formulae there as well. Highly oxygenated functional groups, like those present in the whole sample, ionize more easily in negative ion mode, and it is likely that these low O/C and high H/C compounds that are also present in the whole sample simply could not compete for a charge. The polar fractionation of the acid-soluble portion clearly separates the sample into two distinct fractions. It is obvious that the tannin-like formulae are dominant in the C18 filtrate (Figure 5d), while the lignin-like component dominates the C18 retentate (Figure 5e), with formulae aligning at O/C 0.4-0.7 and H/C 0.5-1.5 being present in both portions. The overlap of formulae in both the filtrate and retentate may indicate that certain components partition into both fractions. However, because FTICR-MS is not distinguishing between structural isomers, it is also probable that the same formulae being detected in both samples are actually different structures that have different polarities that allow them to fractionate into separate portions [23]. The variations in molecular formulae found in hydrophilic versus hydrophobic fractions is consistent with what has been observed previously [23,36]. While significant differences are apparent in these van Krevelen diagrams, PCA is utilized to reveal the more subtle differences that exist based on the relative magnitudes corresponding to the assigned formulae.

From the 8 samples, 17,388 CHO-only formulae were assigned. When removing the duplicate formulae (i.e., those that were common to more than 1 sample), a unique list of 3751 formulae existed. Figure 6a shows a frequency plot demonstrating the number (and percentage) of formulae detected either uniquely to 1 sample or commonly amongst a number of samples. These 3751 formulae account for 84-91% of the total magnitude of all formulae assigned per sample. About 15% of these

Sleighter *et al. Chemical and Biological Technologies in Agriculture* (2015) 2:9

Page 12 of 19

Table 3 Average (by number and magnitude-weighted) mass spectral characteristics for each sample

Sample	O/C		H/C		DBE		DBE/C		%CHO		%CHON		%CHOS	
	num	mag	num	mag	num	mag	num	mag	num	mag	num	mag	num	mag
Whole	0.58	0.61	0.91	0.87	12.9	12.9	0.60	0.62	69%	87%	17%	8%	13%	5%
Acid insoluble	0.37	0.37	0.95	0.95	13.2	12.9	0.57	0.57	82%	87%	16%	11%	2%	2%
Acid soluble	0.57	0.60	0.94	0.91	12.5	12.5	0.58	0.60	70%	87%	19%	9%	11%	4%
C18 Fil:Ret 100:0	0.64	0.67	0.91	0.89	11.7	11.6	0.61	0.61	64%	84%	21%	9%	15%	7%
C18 Fil:Ret 75:25	0.57	0.60	0.94	0.90	12.3	12.3	0.58	0.60	73%	88%	18%	8%	9%	3%
C18 Fil:Ret 50:50	0.53	0.55	0.96	0.94	12.4	12.4	0.57	0.58	76%	90%	17%	7%	7%	2%
C18 Fil:Ret 25:75	0.51	0.51	0.97	0.96	12.8	12.7	0.56	0.57	75%	91%	17%	7%	8%	2%
C18 Fil:Ret 0:100	0.45	0.46	0.96	0.97	14.1	13.6	0.56	0.56	75%	91%	18%	7%	6%	2%

DBE (double bond equivalents) = $(2c + 2 + n + p - h)/2$ for any formula $C_cH_hO_oN_nS_sP_p$
DBE/C: double bond equivalents normalized to the number of carbon atoms in the formula
num indicates that the value given in number-averaged
mag indicates that the value given in magnitude-weighted
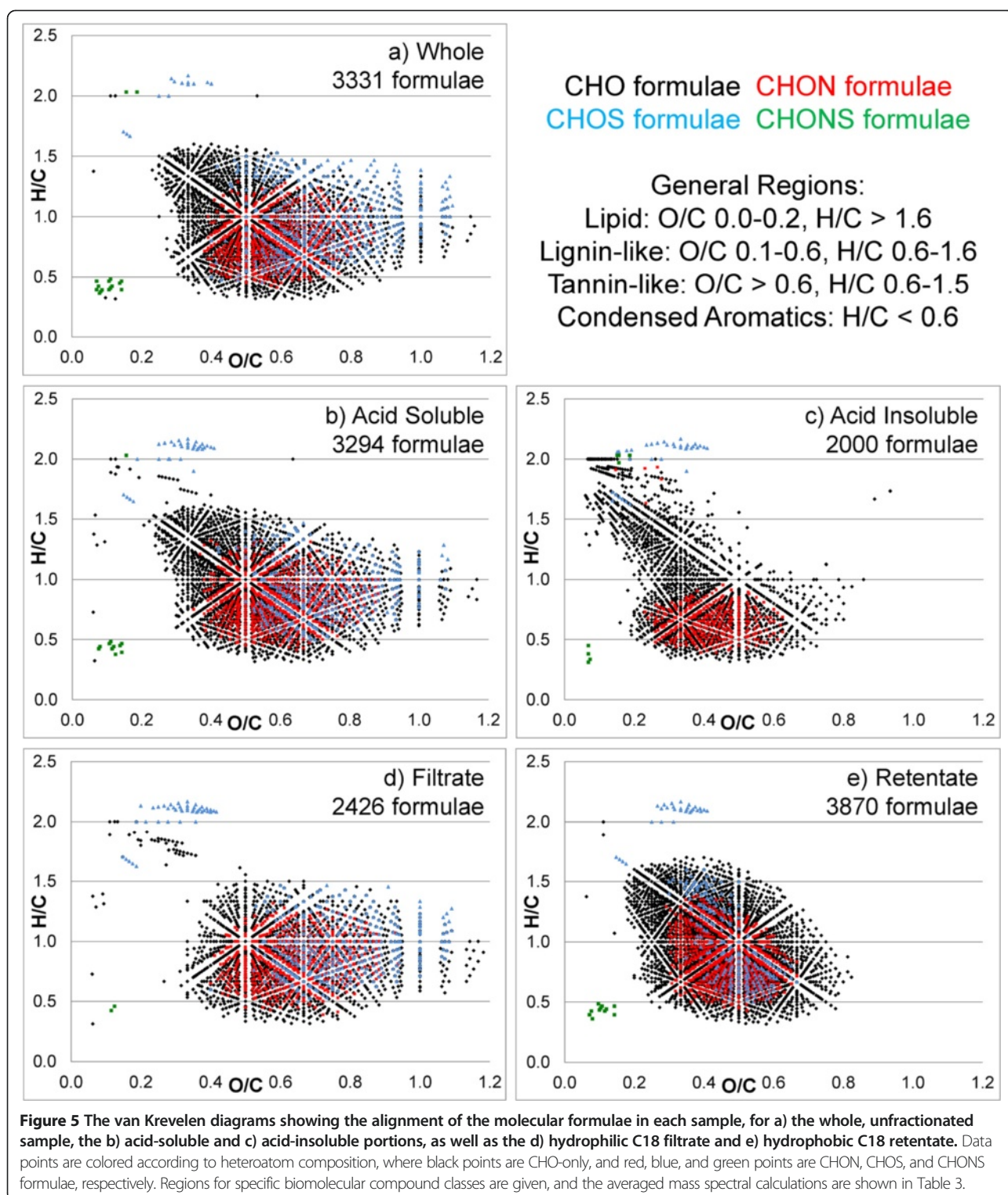The van Krevelen diagrams are shown in Figure 5.

formulae are detected in all 8 samples, while 35% of the formulae are detected in 6–7 samples, indicating that there is a high percentage of commonality amongst some samples. Conversely, about 22% of formulae are detected in only 1 sample, as highlighted by the van Krevelen diagram in Figure 6b. Most of these unique formulae have low O/C ratios and are detected only in the acid-insoluble sample. As discussed above, we would have expected to detect these formulae in the whole sample as well, but these low O/C compounds do not ionize efficiently enough in negative ion mode amongst the lignin- and tannin-like compounds present in the whole sample to enable their detection. The formulae in all 8 samples (Figure 6c) cluster together in the low H/C (mostly <1) region where the lignin- and tannin-like groups meet at O/C 0.4-0.7. The overlap of formulae in numerous samples that have been fractionated (either by pH or polarity) is not necessarily unexpected. As mentioned above, FTICR-MS is not distinguishing between structural isomers, and formulae being detected in multiple samples may have different structures that allow them to fractionate into separate portions, but this structural differentiation is not recognized by FTICR-MS.

The relative magnitudes of these 3751 formulae are used as variables in the FTICR-MS PCA, and Figures 6d and e show the biplots of the samples' scores and the variables' loadings, respectively. PC1 explains 46% of the variance, while PC2 explains an additional 36%. In general, PC1 separates the C18 samples according to polarity, with the filtrate-dominated samples having high positive PC1 scores and the retentate-dominated samples having high negative PC1 scores. The whole and acid-soluble samples fall very closely to the filtrate: retentate 75:25 sample, which approximates the relative proportions of the filtrate and retentate in the acid-soluble sample (Figure 1). The acid-insoluble sample

separates from the other samples with high negative PC1 and PC2 scores. The corresponding van Krevelen diagram, colored according to the boxes drawn in Figure 6e, is shown in Figure 6 f. Formulae in purple (with high positive PC1 loadings) are enriched in the whole, acid-soluble, and filtrate-dominated samples (that have high positive PC1 scores), and these formulae fall mostly in the tannin-like region with high O/C values (Table 4). The green formulae (with both high negative PC1 loadings and high positive PC2 loadings) are enriched in the retentate-dominated samples (that have scores in the same quadrant) and fall mostly in the lignin-like region. These formulae also have notably higher m/z values (Table 4). The red formulae (with both high negative PC1 and PC2 loadings) are enriched in the acid-insoluble sample and have low O/C values and span the H/C scale. These formulae have lower m/z values, indicating that the smaller molecules are first to precipitate out of solution under acidic conditions.

Bioassays and Plant Response

Corn plants (*Zea mays* L.) treated with foliar applications of the 8 samples at 0.01 and 0.1 mg/L C were compared to the control (that was treated with UHQ water). For all assessments (root and shoot elongation, fresh and dry masses), the whole and acid-soluble samples all gave plant growth responses that were statistically better (or at least observably higher) than the control for both carbon rates (Table 5, Figure 7). The whole sample at both concentrations was statistically better than the control for shoot elongation, and the acid-soluble sample at 0.01 mg/L C gave the highest shoot elongation of any of the samples analyzed. The acid-insoluble sample was not statistically different from the control for shoot elongation, but did give a value higher (but not statistically better) than the control for the application at 0.1 mg/L C. For the C18 fractionated samples, the filtrate: retentate

Sleighter *et al. Chemical and Biological Technologies in Agriculture* (2015) 2:9

Page 13 of 19

Figure 5 The van Krevelen diagrams showing the alignment of the molecular formulae in each sample, for a) the whole, unfractionated sample, the b) acid-soluble and c) acid-insoluble portions, as well as the d) hydrophilic C18 filtrate and e) hydrophobic C18 retentate. Data points are colored according to heteroatom composition, where black points are CHO-only, and red, blue, and green points are CHON, CHOS, and CHONS formulae, respectively. Regions for specific biomolecular compound classes are given, and the averaged mass spectral calculations are shown in Table 3.

mixture of 100:0 gave the highest shoot elongations and dry shoot masses at both DOC values, while the other mixtures (75:25, 50:50, 25:75, and 0:100) were not statistically different from the control for shoot elongation or dry shoot mass. Based on these results, it seems that

hydrophilic samples are most influential on shoot development, as the acid-soluble portion performed better than the acid-insoluble portion (which is less oxygenated and more hydrophobic), and the 100:0 hydrophilic filtrate : hydrophobic retentate gave higher shoot measurements
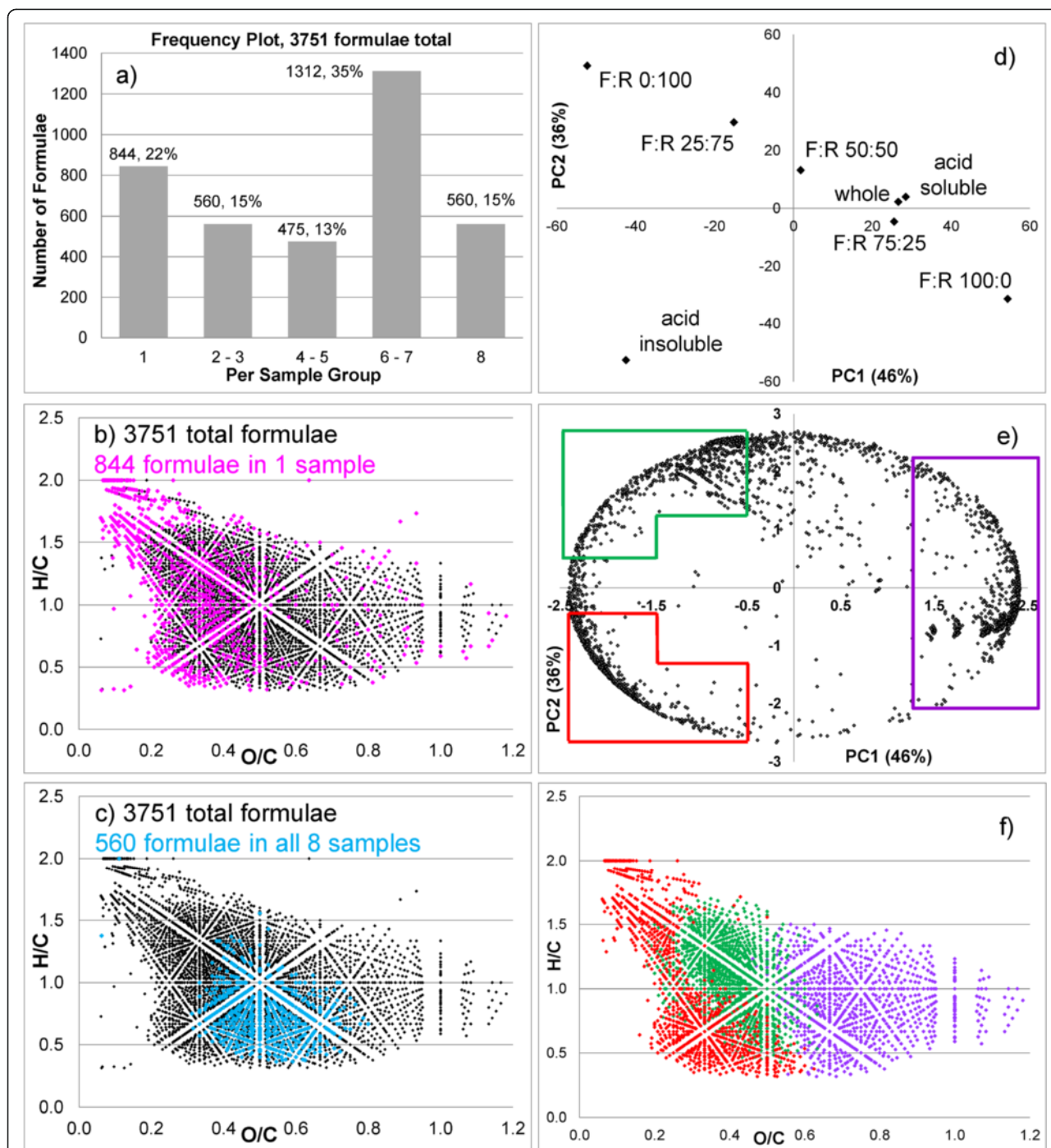
Sleighter *et al. Chemical and Biological Technologies in Agriculture* (2015) 2:9

Page 14 of 19

Figure 6 Molecular formula characteristics and results of the principal component analysis of the FTICR-MS data. Formulae were grouped **a)** in a frequency plot to show the number of formulae that were detected in each of the various samples. The van Krevelen diagrams in panels **b)** and **c)** show all 3751 unique formulae in black points compared to **b)** the 844 formulae unique to any single sample (pink) and to **c)** the 560 formulae common to all 8 samples (blue). The PCA biplot shows the **d)** samples' scores and **e)** variables' loadings, along with **f)** the van Krevelen diagram color-coded according to the boxes drawn in the loadings biplot. Specific characteristics of the formulae responsible for the PCA variance are given in Table 4.

Sleighter *et al. Chemical and Biological Technologies in Agriculture* (2015) 2:9

Page 15 of 19

Table 4 Mass spectral characteristics of the formulae responsible for the variance in the FTICR-MS PCA dataset

Parameter	General characteristics of molecular formulae from PCA					
	Purple (enriched in filtrate-dominated samples)		Green (enriched in retentate-dominated samples)		Red (enriched in acid insoluble)	
	range	average	range	average	range	average
O/C	0.40-1.18	0.74	0.18-0.63	0.40	0.06-0.63	0.29
H/C	0.32-1.50	0.90	0.43-1.70	1.10	0.32-2.00	0.99
DBE	4-20	11.2	4-26	14.1	1-26	13.1
DBE/C	0.31-0.89	0.61	0.20-0.82	0.49	0.03-0.89	0.55
m/z	233-683	451	277-699	559	227-665	429

The PCA scores and loadings are given in Figure 6d and 6e, respectively, with the corresponding color-coded van Krevelen plot shown in Figure 6 f.

than any of the samples containing the retentate. Although only 3 of the shoot measurements were statistically better than the control, 2 of these values were at the lower carbon rate of 0.01 mg/L C. While stimulation can be observed for the shoot measurements, the root system is the principal target of the fertilizer effect and these measurements demonstrate the enhanced plant growth best (as observed in previous studies as well [4-6]).

In general, the lower DOC rate (0.01 mg/L C) gave higher root elongation values, in comparison to the higher DOC rate of 0.1 mg/L C (Table 5, Figure 7). The whole, acid-soluble, and acid-insoluble samples all gave root elongation values higher than the control for both DOC rates, but none were statistically better. For the C18 fractionation samples, the 50:50 and 25:75 mixtures of the filtrate : retentate gave the highest root elongations. In regard to dry root mass, the whole sample was better, but not statistically, than the control for both DOC treatments, but the acid-soluble and acid-insoluble gave root masses that were statistically better (more so for the lower DOC rate). In this case, the acid-insoluble portion that is more hydrophobic gave the best results for the samples fractionated by pH. However, the samples fractionated by polarity display the most interesting trends for the dry root mass measurements of the bioassay. At the lower DOC rate of 0.01 mg/L C, the root masses increased as the C18 mixed samples became dominated by the hydrophobic retentate. The 100:0 filtrate : retentate sample had higher dry root mass than the control (but not statistically better), while the other 4 samples (75:25, 50:50, 25:75, 0:100 filtrate : retentate) were all statistically better and increased in that order. The opposite is true for the higher DOC rate of 0.1 mg/L C, where root mass increased as the samples became dominated by the hydrophilic filtrate. In this case, all 5 mixed samples gave root masses statistically better than the control, but the order here was reversed, where 100:0 filtrate : retentate yielded the highest root mass. It should also be noted that while all of the C18 fractionation samples gave positive results for dry root mass,

they largely gave lower dry shoot masses than the control (but not statistically worse), except for the 100:0 filtrate : retentate sample that gave higher dry shoot masses than the control. It is evident that the application was taken up easily by the foliage and that it impacted the root system most.

The results presented here are a good example highlighting that plant response is due to not only the amount of carbon applied but also the type (i.e., fraction) of carbon. Certain parts of the plant (root vs. shoot) appear to respond differently to various types of carbon (hydrophilic vs. hydrophobic). These types of contradictory effects have also been reported in other studies [6,15-18]. While the focus for this foliar application was on the amount and type of carbon, it is likely that the trace metals and other micronutrients naturally present in the DOM also play an active role in enhancing plant growth [46-48]. In some cases, the hydrophilic samples (i.e., the acid-soluble or filtrate-dominated samples) gave the best plant response (i.e., shoot elongation and dry shoot mass at both DOC rates, dry root mass for the filtrate-dominated samples at the higher DOC rate of 0.1 mg/L C). These hydrophilic samples also have the highest Fe content. Other times the hydrophobic samples (i.e., the acid-insoluble or retentate-dominated samples) were better (i.e., dry root mass, especially for the retentate dominated samples at the lower DOC rate of 0.01 mg/L C). The acid-insoluble portion contains less Fe than the acid-soluble sample, but still has a significant Fe concentration, whereas the hydrophobic C18 retentate is nearly void of Fe. In general, the hydrophobic samples have lower Fe contents. It has yet to be determined whether these plant responses are due to the type of carbon components in each of these fractions (i.e., hydrophilic polar vs. hydrophobic non-polar) or due to the varying concentrations of Fe and other micronutrients that are also present. While more research is necessary to discern the mechanism(s) responsible for these observations, this study is an example of enhanced plant growth during controlled application of humic substances that vary in their chemical components and

Sleighter *et al. Chemical and Biological Technologies in Agriculture* (2015) 2:9

Page 16 of 19

Table 5 Results of the bioassays employing foliar applications of the 8 samples at 2 carbon rates

Sample	Length (cm)		Fresh weight (g)	Dry Weight (mg)	
	Root	Shoot		Root	Shoot
Control	32.7 ± 3.5	28.2 ± 3.9	27.4	155 ± 19	95 ± 36
Whole, 0.01 mg/L C	**33.0 ± 3.6**	***32.6 ± 4.3***	**30.4**	**165 ± 31**	**118 ± 23**
	(0.881)	***(0.028)***		**(0.437)**	**(0.111)**
Acid soluble, 0.01 mg/L C	**36.2 ± 5.5**	***34.1 ± 3.4***	**32.8**	***189 ± 25***	**125 ± 35**
	(0.115)	***(0.002)***		***(0.004)***	**(0.085)**
Acid insoluble, 0.01 mg/L C	**36.4 ± 8.0**	27.8 ± 3.2	**28.0**	***221 ± 37***	**108 ± 25**
	(0.197)	(0.800)		***(0.0001)***	**(0.383)**
100:0 Filt : Ret, 0.01 mg/L C	***37.0 ± 3.3***	**30.6 ± 3.9**	**29.5**	**184 ± 20**	**111 ± 32**
	(0.011)	**(0.190)**		**(0.108)**	**(0.332)**
75:25 Filt : Ret, 0.01 mg/L C	**35.5 ± 5.6**	27.9 ± 6.4	25.7	***192 ± 53***	89 ± 36
	(0.203)	(0.894)		***(0.045)***	(0.685)
50:50 Filt : Ret, 0.01 ppm	***38.3 ± 4.4***	27.5 ± 3.6	27.4	***219 ± 21***	92 ± 21
	(0.006)	(0.668)		***(0.0001)***	(0.777)
25:75 Filt : Ret, 0.01 mg/L C	***38.8 ± 5.5***	26.3 ± 3.3	25.5	***221 ± 39***	84 ± 20
	(0.008)	(0.243)		***(0.0001)***	(0.399)
0:100 Filt : Ret, 0.01 mg/L C	**36.4 ± 3.1**	27.0 ± 3.5	**28.4**	***231 ± 24***	98 ± 25
	(0.062)	(0.457)		***(0.00004)***	(0.882)
Whole, 0.1 mg/L C	**33.0 ± 1.9**	***32.1 ± 4.1***	**29.5**	**160 ± 14**	**112 ± 28**
	(0.809)	***(0.044)***		**(0.537)**	**(0.260)**
Acid soluble, 0.1 mg/L C	**35.5 ± 5.5**	**31.1 ± 2.5**	**29.3**	**173 ± 25**	**112 ± 23**
	(0.202)	**(0.063)**		**(0.102)**	**(0.247)**
Acid insoluble, 0.1 mg/L C	**36.6 ± 5.6**	**29.1 ± 4.4**	**28.6**	***204 ± 30***	**113 ± 39**
	(0.078)	**(0.634)**		***(0.0005)***	**(0.313)**
100:0 Filt : Ret, 0.1 mg/L C	32.0 ± 3.5	**29.2 ± 5.0**	**32.3**	***229 ± 40***	**118 ± 36**
	(0.638)	**(0.645)**		***(0.0001)***	**(0.185)**
75:25 Filt : Ret, 0.1 mg/L C	31.9 ± 3.7	26.5 ± 4.1	26.8	***214 ± 31***	98 ± 29
	(0.607)	(0.342)		***(0.0001)***	(0.872)
50:50 Filt : Ret, 0.1 mg/L C	***37.2 ± 5.5***	26.8 ± 4.0	25.7	***214 ± 37***	90 ± 22
	(0.041)	(0.430)		***(0.0003)***	(0.697)
25:75 Filt : Ret, 0.1 mg/L C	**33.2 ± 3.8**	27.9 ± 4.4	**27.5**	***195 ± 61***	105 ± 33
	(0.764)	(0.862)		***(0.006)***	(0.561)
0:100 Filt : Ret, 0.1 mg/L C	31.7 ± 5.6	26.3 ± 3.5	26.1	***202 ± 45***	90 ± 23
	(0.621)	(0.253)		***(0.007)***	(0.691)

Average values (with the standard deviations) of the 10 individual measurements for each treatment are given for the root and shoot measurements. The fresh weight of all seedlings for a given treatment were taken together to give one measurement. Values in bold indicate a response observably higher than the control, and values in bold-italic indicate a response statistically better than the control. P values are given in parentheses for each measurement. Visual depictions of the root and shoot values are shown in Figure 7.

concentrations. Future studies that alter the DOC and micronutrient rates in a systematic manner will provide an enhanced understanding of this likely synergistic plant stimulation. Moreover, the application method (foliar in this case) may play a key role in determining the plant responses. Thus, other types of applications (such as seed treatment and soil application) are also being investigated.

Conclusions

The acid-insoluble component accounted for 43% of the carbon and 31% of the iron of the whole sample. After extraction of the acid-soluble portion, the C18 retentate portion contained 36% and 4% of the carbon and iron, respectively, while the remaining (and majority of) carbon and iron was found in the filtrate portion. The whole and acid-soluble samples were very similar, as
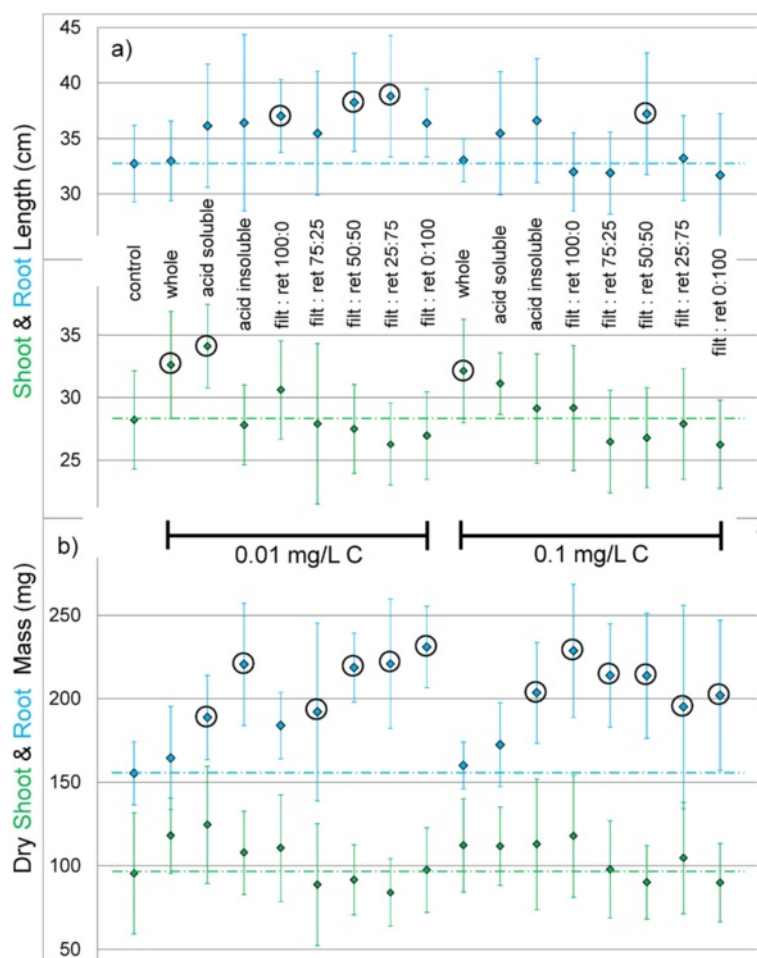
Sleighter *et al. Chemical and Biological Technologies in Agriculture* (2015) 2:9

Page 17 of 19

Figure 7 Results of the bioassays employing foliar applications of the 8 samples at 2 carbon rates. The DOC rates used were 0.01 and 0.1 mg/L C, and the average **a)** shoot and root lengths (cm) and **b)** dry shoot and root masses (mg) for all seedlings are given. Shoot measurements are given in green, while root measurements are given in blue. Error bars are the standard deviations of the 10 individual measurements for each treatment. Circles around data points indicate that the data point is statistically better ($p \leq 0.05$) than the control. The dotted lines across the plot indicate the control average for each type of measurement. Actual measurements and p values are given in Table 5.

characterized by NMR and FTICR-MS. The acid-insoluble sample was very low in oxygen and was mostly aromatic, but still contained a significant portion of aliphatics. A clear shift in the chemical composition was observed for the C18 samples, where the filtrate and retentate samples were mixed at ratios of filtrate : retentate 100:0, 75:25, 50:50, 25:75, and 0:100. As more retentate was added, the O/C ratios decreased while the DBE increased (with H/C not changing significantly). The tannin-like component dominates the filtrate portion, while the lignin-like component dominates the retentate portion, due to the differences in their polarity and hydrophobicity. PCA assisted in revealing the more subtle differences between the whole sample fractionated according to pH, as well as the acid-soluble portion fractionated using C18 resin to obtain the filtrate and retentate samples.

Bioassays using foliar applications of the 8 samples at 0.01 and 0.1 mg/L C demonstrated that plant responses are not only due to the amount of carbon but also due to the type of carbon present. Samples of a more hydrophilic nature (those that are most oxygenated as revealed by the NMR and FTICR-MS analysis) yielded the highest response for the shoot measurements. However, the root measurements were more responsive than the shoot. The lower DOC rate of 0.01 mg/L C in general gave higher root elongation values than the higher DOC rate of 0.1 mg/L C. The acid-insoluble and acid-soluble portions individually gave higher root elongation and larger root masses than the whole sample and the control, with the hydrophobic, less oxygenated acid-insoluble sample performing better. Based on dry root masses, the C18 polarity fractions showed that larger root systems occurred when there was more hydrophobic material

present at the lower carbon application (0.01 mg/L C). The opposite was true for the root system at the higher carbon application (0.1 mg/L C), where larger roots existed when more hydrophilic material was present. This study clearly demonstrates that plant growth can be improved by the controlled application of humic substances that vary in their chemical components and concentrations. However, mechanisms for these enhancements remain unclear. Further work is necessary to discern whether the DOC type and concentration are responsible for the improved plant growth or whether micronutrients are more significant, but it is likely a combined effect in which both variables are important.

References
1. Aiken GR, MacCarthy P, Malcolm RL, Swift RS (1985) Humic Substances in Soil, Sediment, and Water. Wiley, New York
2. Stevenson JF (1994) Humus Chemistry: Genesis, Composition, Reactions. Wiley, New York
3. Perdue EM, Ritchie JD (2003) Dissolved organic matter in freshwaters. In: Drever JI (ed) Treatise on Geochemistry: Surface and Ground Water, Weather, and Soils, volume 5. Elsevier, Oxford
4. Chen Y, Aviad T (1990) Effects of humic substances on plant growth. In: MacCarthy P, Clapp CE, Malcolm RL, Bloom RR (ed) Humic Substances in Soil and Crop Sciences: Selected Readings. American Society of Agronomy, Madison
5. Nardi S, Pizzeghello D, Muscolo A, Vianello A (2002) Physiological effects of humic substances on higher plants. Soil Biol Biochem 34:1527–1536
6. Rose MT, Patti AF, Little KR, Brown AL, Jackson WR, Cavagnaro TR (2014) A meta-analysis and review of plant growth response to humic substances: Practical implications for agriculture. In: Sparks DL (ed) Advances in Agronomy, volume 124. Elsevier, San Diego
7. Canellas LP, Olivares FL, Okorokova-Facanha AL, Racanha AR (2002) Humic acids isolated from earthworm compost enhance root elongation, lateral root emergence, and plasma membrane H$^+$-ATPase activity in maize roots. Plant Physiol 130:1951–1957
8. Pascual JA, Garcia C, Hernandez T, Lerma S, Lynch JM (2002) Effectiveness of municipal waste compost and its humic fraction in suppressing *Pythium ultimum*. Microb Ecol 44:59–68
9. Chen Y, De Nobili M, Aviad T (2004) Stimulatory effects of humic substances on plant growth. In: Magdoff F, Weil RR (ed) Soil organic matter in sustainable agriculture. CRC Press, Boca Raton
10. Zandonadi DB, Canellas LP, Facanha AR (2007) Indolacetic and humic acids induce lateral root development through a concerted plasmalemma and tonoplast H$^+$ pumps activation. Planta 225:1583–1595
11. Loffredo E, Berloco M, Senesi N (2008) The role of humic fractions from soil and compost in controlling the growth in vitro of phytopathogenic and antagonistic soil-borne fungi. Ecotox Environ Safe 69:350–357
12. Ferrara G, Brunetti G (2010) Effects of the times of application of a soil humic acid on berry quality of table grape (*Vitis vinifera* L.) cv Italia. Span J Agric Res 8:817–822
13. Silva-Matos RRS, Cavalcante IHL, Junior GBS, Albano FG, Cunha MS, Beckmann-Cavalcante (2012) Foliar spray of humic substances on seedling production of watermelon cv. Crimson Sweet. J Agron 11: 60–64
14. Hertkorn N, Ruecker C, Meringer M, Gugisch R, Frommberger M, Perdue EM, Witt M, Schmitt-Kopplin P (2007) High-precision frequency measurements: Indispensable tools at the core of the molecular-level analysis of complex systems. Anal Bioanal Chem 389:1311–1327
15. Muscolo A, Sidari M, Nardi S (2013) Humic substance: Relationship between structure and activity. Deeper information suggests univocal findings. J Geochem Explor 129:57–63
16. Nardi S, Muscolo A, Vaccaro S, Baiano S, Spaccini R, Piccolo A (2007) Relationship between molecular characteristics of soil humic fractions and glycolytic pathway and krebs cycle in maize seedlings. Soil Biol Biochem 39:3138–3146
17. Canellas LP, Spaccini R, Piccolo A, Dobbss LB, Okorokova-Facanha AL, de Araujo SG, Olivares FL, Facanha AR (2009) Relationships between chemical characteristics and root growth promotion of humic acids isolated from Brazilian Oxisols. Soil Sci 174:611–620
18. Dobbss LB, Canellas LP, Olivares FL, Aguiar NO, Peres LEP, Axevedo M, Spaccini R, Piccolo A, Facanha AR (2010) Bioactivity of chemically transformed humic matter from vermicompost on plant root growth. J Agric Food Chem 58:3681–3688
19. Thurman EM, Malcolm RL (1981) Preparative isolation of aquatic humic substances. Environ Sci Technol 15:463–466
20. Koch BP, Ludwichowski K-U, Kattner G, Dittmar T, Witt MR (2008) Advanced characterization of marine dissolved organic matter by combining reversed-phase liquid chromatography and FT-ICR-MS. Mar Chem 111:233–241
21. Stenson AC (2008) Reversed-phase chromatography fractionation tailored to mass spectral characterization of humic substances. Environ Sci Technol 42:2060–2065
22. Liu Z, Sleighter RL, Zhong J, Hatcher PG (2011) The chemical changes of DOM from black waters to coastal marine waters by HPLC combined with ultrahigh resolution mass spectrometry. Estuar Coast Shelf Sci 92:205–216
23. Sleighter RL, Hatcher PG (2008) Molecular characterization of dissolved organic matter (DOM) along a river to ocean transect of the lower Chesapeake Bay by ultrahigh resolution electrospray ionization Fourier transform ion cyclotron resonance mass spectrometry. Mar Chem 110:140–152
24. McKnight DM, Boyer EW, Westerhoff PK, Doran PT, Kulbe T, Andersen DT (2001) Spectrofluorometric characterization of dissolved organic matter for indication of precursor organic material and aromaticity. Limnol Oceanogr 46:38–48
25. Fellman JB, Hood E, Spencer RGM (2010) Fluorescence spectroscopy opens new windows into dissolved organic matter dynamics in freshwater ecosystems: A review. Limnol Oceanogr 55:2452–2462
26. Lam B, Simpson AJ (2008) Direct ^{1}H NMR spectroscopy of dissolved organic matter in natural waters. Analyst 133:263–269
27. Gaskell SJ (1997) Electrospray: principles and practice. J Mass Spectrom 32:677–688
28. Cech NB, Enke CG (2001) Practical implications of some recent studies in electrospray ionization fundamentals. Mass Spectrom Rev 20:362–387
29. Marshall AG, Hendrickson CL, Jackson GS (1998) Fourier transform ion cyclotron resonance mass spectrometry: A primer. Mass Spectrom Rev 17:1–35
30. Dittmar T, Koch B, Hertkorn N, Kattner G (2008) A simple and efficient method for the solid phase extraction of dissolved organic matter (SPE-DOM) from seawater. Limnol Oceanogr Meth 6:230–235
31. Weishaar JL, Aiken GR, Bergamaschi BA, Fram MS, Fujii R, Mopper K (2003) Evaluation of specific ultraviolet absorbance as an indicator of the chemical composition and reactivity of dissolved organic carbon. Environ Sci Technol 37:4702–4708
32. Cory RM, Miller MP, McKnight DM, Guerard JJ, Miller PL (2010) Effect of instrument-specific response on the analysis of fulvic acid fluorescence spectra. Limnol Oceanogr Meth 8:67–78
33. Sleighter RL, McKee GA, Liu Z, Hatcher PG (2008) Naturally present fatty acids as internal calibrants for Fourier transform mass spectra of dissolved organic matter. Limnol Oceanogr Meth 6:246–253

Sleighter *et al. Chemical and Biological Technologies in Agriculture* (2015) 2:9

Page 19 of 19

34. Sleighter RL, Chen H, Wozniak AS, Willoughby AS, Caricasole P, Hatcher PG (2012) Establishing a measure of reproducibility of ultrahigh-resolution mass spectra for complex mixtures of natural organic matter. Anal Chem 84:9184–9191

35. Stubbins A, Spencer RGM, Chen H, Hatcher PG, Mopper K, Hernes PJ, Mwamba VL, Mangangu AM, Wabakanghanzi JN, Six J (2010) Illuminated darkness: Molecular signatures of Congo River dissolved organic matter and its photochemical alteration as revealed by ultrahigh precision mass spectrometry. Limnol Oceanogr 55:1467–1477

36. Sleighter RL, Liu Z, Xue J, Hatcher PG (2010) Multivariate statistical approaches for the characterization of dissolved organic matter analyzed by ultrahigh resolution mass spectrometry. Environ Sci Technol 44:7576–7582

37. Helms JR, Stubbins A, Ritchie JD, Minor EC, Kieber DJ, Mopper K (2008) Absorption spectral slopes and slope ratios as indicators of molecular weight, source, and photobleaching of chromophoric dissolved organic matter. Limnol Oceanogr 53:955–969

38. Reemtsma T (2009) Determination of molecular formulas of natural organic matter molecules by (ultra-) high-resolution mass spectrometry: Status and needs. J Chromatogr A 1216:3687–3701

39. Sleighter RL, Hatcher PG (2011) Fourier transform mass spectrometry for the molecular level characterization of natural organic matter: Instrument capabilities, applications, and limitations. In: Nikolic G (ed) Fourier Transforms- Approach to Scientific Principles. InTech, Vienna. available from: http://www.intechopen.com/articles/show/title/fourier-transform-mass-spectrometry-for-the-molecular-level-characterization-of-natural-organic-matt

40. Stenson AC, Landing WM, Marshall AG, Cooper WT (2002) Ionization and fragmentation of humic substances in electrospray ionization Fourier transform-ion cyclotron resonance mass spectrometry. Anal Chem 74:4397–4409

41. Kim S, Kramer RW, Hatcher PG (2003) Graphical method for analysis of ultrahigh-resolution broadband mass spectra of natural organic matter, the van Krevelen diagram. Anal Chem 75:5336–5344

42. Hockaday WC, Purcell JM, Marshall AG, Baldock JA, Hatcher PG (2009) Electrospray and photoionization mass spectrometry for the characterization of organic matter in natural waters: a qualitative assessment. Limnol Oceanogr Meth 7:81–95

43. Ohno T, He Z, Sleighter RL, Honeycutt CW, Hatcher PG (2010) Ultrahigh resolution mass spectrometry and indicator species analysis to identify marker components of soil- and plant biomass- derived organic matter fractions. Environ Sci Technol 44:8594–8600

44. Sleighter RL, Cory RM, Kaplan LA, Abdulla HAN, Hatcher PG (2014) A coupled geochemical and biogeochemical approach to characterize the bioreactivity of dissolved organic matter from a headwater stream. J Geophys Res Biogeosci 119:1520–1537

45. Ikeya K, Sleighter RL, Hatcher PG, Watanabe A (2012) Compositional features of Japanese Humic Substances Society standard soil humic and fulvic acids by Fourier transform ion cyclotron resonance mass spectrometry and X-ray diffraction profile analysis. Humic Substances Res 9:25–33

46. Pinton R, Cesco S, De Nobili M, Santi S, Varanini Z (1998) Water- and pyrophosphate-extractable humic substances fractions as a source of iron for Fe-deficient cucumber plants. Biol Fert Soils 26:23–27

47. Chen Y, Clapp CE, Magen H (2004) Mechanisms of plant growth stimulation by humic substances: The role of organo-iron complexes. Soil Sci Plant Nutr 50:1089–1095

48. Santiago A, Delgado A (2007) Effects of humic substances on iron nutrition of lupin. Biol Fert Soils 43:829–836